A screen of FDA-approved drugs with minigenome identified tigecycline as an antiviral targeting nucleoprotein of Crimean-Congo hemorrhagic fever virus

Authors: Minato Hirano[1)], Yasuteru Sakurai[1) 2)], Shuzo Urata[1) 2)], Yohei Kurosaki[1) 2)], Jiro Yasuda[1) 2)], Kentaro Yoshii[1) 2)]

1) National Research Center for the Control and Prevention of Infectious Diseases, Nagasaki University, Nagasaki, Japan
2) Department of Emerging Infectious Diseases, Institute of Tropical Medicine (NEKKEN), Nagasaki University, Nagasaki, Japan

Corresponding author: Kentaro Yoshii,
Postal address: 1-12-4 Sakamoto, Nagasaki City 852-8523, Japan
Tel/fax: +81-95-819-8595
E-mail: kyoshii@nagasaki-u.ac.jp

Abstract

Crimean-Congo hemorrhagic fever virus (CCHFV) belongs to the genus *Orthonairovirus* and is the causative agent of a viral hemorrhagic disease with a case fatality rate of 30%. However, limited studies have been conducted to explore antiviral compounds specific to CCHFV. In this study, we developed a minigenome system of orthonairoviruses, CCHFV and Hazara virus to analyze viral replication and screened an FDA-approved compound library. The transfection of the minigenome components induced marked increase in luciferase expression, indicating the sufficient replication and translation of reporter RNA. Compound library screening identified 14 candidate compounds that significantly decreased luciferase activity. Some of the compounds also inhibited the replication of the infectious Hazara virus. The mechanism of inhibition by tigecycline was further analyzed, and a decrease in the interaction between the viral N protein and RNA by tigecycline was observed. This work provides a basis for validation using animal models and the design of chemical derivatives with stronger activity in future studies on the development of an antiviral against CCHFV.

Keywords:

Crimean-Congo hemorrhagic fever virus, Minigenome, Drug screening, Tigecycline, Nucleoprotein

Highlights:

- Minigenome of CCHFV Hoti strain and HAZV JC280 strain was developed.
- Library screening of FDA-approved compounds identified 14 candidate compounds.
- Compounds including tigecycline showed inhibition at 10 μM concentration.
- Tigecycline treatment dissociated the interaction between CCHFV N protein and RNA: a new target of antiviral development.

1. Introduction

Crimean-Congo hemorrhagic fever virus (CCHFV) belongs to the genus *Orthonairovirus* and has tri-segmented negative-sense RNAs as genome (Bente et al., 2013; Knipe and Howley, 2013). S, M, and L segments of the viral genomic RNAs encode nucleoprotein (N), glycoprotein precursor, and large (L) protein, respectively. The 5' and 3' non-coding sequences (NCS) of the genomic RNAs are essential for genome replication and acting as a promoter that is recognized by viral L protein for the synthesis of complementary strands (Flick et al., 2003; Matsumoto et al., 2019). N and viral genomic RNA form filamentous ribonucleoprotein complexes (Wang et al., 2016). L has RNA-dependent RNA polymerase (RdRp) activity for the synthesis of mRNA and complementary RNA (Devignot et al., 2015; Mirza et al., 2019). In a recent study, the ovarian tumor protease domain of L was found to regulate the host innate immune response (Scholte et al., 2017). The interaction between N and L is essential for viral genome replication (Macleod et al., 2015).

CCHFV is an arthropod-borne virus, or arbovirus (Bente et al., 2013; Spengler et al., 2016) and is widely distributed in Africa, the Middle East, southern Europe, and Asia, overlapping with the distribution of the major tick vector, *Hyalomma* spp. (Bente et al., 2013). CCHFV is the causative agent of Crimean-Congo hemorrhagic fever (CCHF), a viral hemorrhagic disease with a case fatality rate of 30%. Humans can be infected through tick bites or exposure to the blood or tissue of infected animals (Bente et al., 2013). Human-to-human transmission has also been reported among healthcare workers in patient care (Altaf et al., 1998; Maltezou et al., 2009). After three to seven days of incubation, CCHF begins to manifest influenza-like symptoms and develops into hemorrhage and acute liver and kidney failure, followed by sharp mood swings and confusion (Akıncı et al., 2013; Bente et al., 2013). Disease outcome in CCHF has been correlated with the

level of viremia, decreased platelet counts, elevated liver enzymes, and others (Akıncı et al., 2013).

The treatment of patients with CCHF is primarily supportive, and there is currently no FDA-approved vaccine or specific antiviral therapeutics (Dai et al., 2021). Ribavirin, a well-known small molecule with broad antiviral activity, has been reported to inhibit viral replication *in vitro* and *in vivo* (Johnson et al., 2018; Paragas et al., 2004; Watts et al., 1989). Additional nucleotide analogs, favipiravir and 2'-deoxy-2'-fluorocytidine, showed antiviral activity (Hawman et al., 2018; Welch et al., 2017); however, their efficacy in clinical settings has yet to be fully evaluated. Due to CCHFV being a biosafety level-4 pathogen, there have been a limited number of studies on targeted antiviral compounds against CCHFV infection and their mechanisms.

The minigenome is an experimental system used to analyze viral replication, including CCHFV, by the exogenous introduction of minimal viral proteins and genomic RNA elements (Bergeron et al., 2010; Hoenen et al., 2011). Viral RNA transcription and translation can be inferred via the expression of a reporter protein encoded in the RNA with viral sequence. It provides high-throughput quantitative data, which is ideal for antiviral screening (Jasenosky et al., 2010; Ozawa et al., 2013). In this study, we developed minigenome systems of CCHFV Hoti strain which was isolated from a patient with the hemorrhagic disease in the Balkans (Duh et al., 2008), and Hazara virus (HAZV), a close relative of CCHFV used as a model of infection (Dowall et al., 2012). Using those systems, we explored antiviral compounds against CCHFV with an FDA-approved compound library.

2. Materials and methods

2.1 Cell culture

Baby hamster kidney-21 (BHK-21) cells were cultured at 37°C in a minimum essential medium (MEM, Fujifilm Labchem Wako, Osaka, Japan) supplemented with 8% (v/v) fetal bovine serum (FBS) and penicillin/streptomycin. Human embryonic kidney 293T (HEK293T) cells and human small-cell carcinoma SW-13 cells were grown at 37°C in Dulbecco's modified Eagle's medium (Fujifilm Labchem Wako) containing 10% (v/v) FBS and penicillin/streptomycin.

2.2 Plasmids and RNA

To construct the pCAG-Hyg-CCHFV L and pCAG-Hyg-HAZV L plasmids, coding sequences (CDS) of the L gene of the CCHFV Kosova Hoti strain (GenBank accession no. **EU044832**) and HAZV JC280 strain (**DQ076419**) were optimized for human codon usage and were synthesized *in vitro* (Integrated DNA Technologies, Inc., Coralville, IA and Azenta Life Sciences, South Plainfield, NJ). These were then subcloned into pCAG-Hyg vector (Fujifilm Labchem Wako). pCAG-Hyg-CCHFV N and pCAG-Hyg-HAZV N were constructed in the same manner. Strep-Tag or His-Tag sequences were inserted at the 3' terminus of the CDS of L or N, respectively. CDS of green fluorescent protein (GFP) with a self-cleavage peptide of thosea asigna virus was inserted upstream of the reading flame of CCHFV N to construct pCAG-Hyg-GFP-T2A-CCHFV N. To construct pGEM-3Z-secNluc with CCHFV L segment NCS and that with HAZV S segment NCS, the CDS of the viral gene was replaced with that of secretory NanoLuc (secNluc) and spacer sequences, and was synthesized *in vitro* (Integrated DNA Technologies). For the synthesis of the reporter RNA, the T7-promoter was inserted upstream of the 5' NCS. pGEM-3Z-mCherry with CCHFV L segment NCS was constructed by the replacement of the CDS with that of mCherry gene. Mutation at the amino acid position of 2517D-to-A was introduced using In-Fusion HD Cloning kit (Takara Bio, Kusatsu, Japan) to construct pCAG-Hyg-CCHFV L (ΔRdRp).

To synthesize reporter RNAs, pGEM-3Z-secNluc with viral NCS was linearized and subjected to transcription using MEGAscript T7 Transcription kit (Thermo Fisher Scientific, Waltham, MA) according to manufacturer's protocol.

2.3 Antibodies, Strep-Tactins, and compounds

Anti-His-tag mAb was purchased from IBA-lifescience (Göttingen, Germany). Anti-His-tag mAb-HRP-DirectT was purchased from Medical & Biological Laboratories Co. (Tokyo, Japan). Anti-GAPDH monoclonal antibody conjugated with peroxidases was purchased from Fujifilm Labchem Wako. Precision Strep Tactin-HRP Conjugate was purchased from Bio-Rad (Hercules, CA).

Minocycline hydrochloride was purchased from Fujifilm Labchem Wako. Tetracycline, doxycycline hyclate, minocycline hydrochloride, tigecycline, dihydroergotamine mesylate, ergotamine tartrate, and promethazine hydrochloride were purchased from Tokyo Chemical Industry (Tokyo, Japan). Minocycline hydrochloride and nisoldipine were purchased from Fujifilm Labchem Wako.

2.4 Virus and viral titration

HAZV JC280 strain (Begum et al., 1970) was kindly provided by Prof. Roger Hewson, Public Health England's Porton Down Institute. The working stock of the virus was propagated in SW-13 cells.

For viral titration, the monolayers of SW-13 cells prepared in multi-well plates were incubated

with serial dilutions of viruses for one hour (h) and were overlaid with MEM containing 2% (v/v) FBS and 0.7% (w/v) UltraPure Agarose (Thermo Fisher Scientific). Following incubation for four days, the cells were fixed with ethanol containing 16% (v/v) acetic acid and stained with 1% (w/v) Amido black in phosphate-buffered saline. Viral titers were expressed as plaque-forming units (PFU)/mL.

2.5 Western blotting

HEK293T cells in 12 well plates were co-transfected with pCAG-Hyg-CCHFV L and pCAG-Hyg-CCHFV N, or those of HAZV using X-tremeGene HP DNA transfection reagent (Merck KGaA, Darmstadt, Germany). At 48 h post-transfection (h.p.t.), the cells were lysed with Cell Lysis Buffer M (Fujifilm Labchem Wako). SDS-PAGE and western blotting were performed with ePAGEL HR Gel (Atto, Tokyo, Japan), anti-His Tag antibody, anti-GAPDH antibody, and Strep-Tactin conjugated with HRP. The bands were visualized with Immobilon Western Chemiluminescent HRP Substrate (Merck) and taken with LuminoGraph I (Atto).

2.6 Minigenome assay and strand-specific reverse transcription and qPCR (RT-qPCR)

HEK293T cells cotransfected with CCHFV or HAZV expression plasmids were further transfected with the reporter RNA using Lipofectamine MessengerMAX (Thermo Fisher Scientific) six hours later. At 24 or 48 h.p.t., luciferase expression was evaluated using Nano-Glo Luciferase Assay System (Promega, Madison, WA) with SpectraMax iD5 (Molecular Devices, San Jose, CA) according to the manufacturer's instructions.

Total RNA was extracted from HEK293T cells with the minigenome at 48 h.p.t. using ISOSPIN Cell&Tissue RNA (Nippon Gene Co., Ltd., Tokyo, Japan). cDNA was synthesized by reverse

transcription using SuperScript III (Thermo Fisher Scientific) and gene-specific primers against mRNAs of secNluc (5'catacggccgtccgaaata3') and GAPDH (5'gcccaatacgaccaaatcc3'). qPCR was conducted using KAPA SYBR FAST qPCR Kit (KAPA Biosystems, Wilmington, MA), primers targeting secNluc (Fw: 5'attgtcctgagcggtgaaa3', Rv: cacagggtacaccaccttaaa3') and GAPDH (Fw: 5'agccacatcgctcagacac3', Rv: 5'gcccaatacgaccaaatcc3'), and StepOnePlus Real Time PCR system (Thermo Fisher Scientific). The relative RNA abundance of the reporter RNA against GAPDH was calculated using the CT value.

2.7 Drug screening

BHK-21 cells with the minigenome were prepared on 96 well plates. At 1.5 h.p.t., compounds of FDA-approved Drug Library, Japan version (Enzo Life Sciences, Farmingdale, NY) or positive control ribavirin were added at a final concentration of 20 μg/ml in the culture medium with 1% (v/v) DMSO. Luciferase assay was conducted at 48 h.p.t., and cell viability was measured using Resazurin Cell Viability Assay Kit (Biotium, Fremont, CA) according to the manufacturer's instructions. After the $\log_{10}$ conversion of luminescence, Dunnett's test of multiple-comparison against DMSO treated samples was conducted to reduce the rate of type II error in the determination of compounds that significantly decreased the luciferase activity. The control plates were used to calculate the Z-factor. To compare the distribution of the data, the data of the treated plates were converted to Robust Z-score, also known as the median absolute deviation method (Chung et al., 2008; Huber and Rochetti, 2009).

2.8 Dose-response analysis and calculation of concentration of 50% Inhibition

BHK-21 cells with the minigenome were prepared, and the compounds were added to the culture medium with 1% (v/v) DMSO at a final concentration from 0 to 50 μM. Luciferase assay was

conducted at 48 h.p.t., and the relative luciferase signal (%) was calculated in relation to the control wells. A fitting curve with non-linear regression was conducted based on triplicate results, and the concentration of 50% inhibition was measured using GraphPad Prism (GraphPad Software, San Diego, CA).

SW-13 cells were infected with HAZV at an multiplicity of infection (MOI) of 0.005 for one h and cultured with the compounds. At 48 h.p.i., the viral titer in the supernatant was measured. The concentration of 50% inhibition was calculated as described above.

2.9 Influence of tigecycline on the binding of N to reporter RNA

HEK293T cells transfected with CCHFV expression plasmids were lysed with Cell Lysis Buffer M at 48 h.p.t. The lysate containing 80 μg of total protein was incubated with 100 μM ribavirin or tigecycline, and the mixture was further incubated with 50 ng of synthesized reporter RNA. To precipitate N, the mixtures were incubated with Cell Lysis Buffer M containing Ab-Capcher Extra beads (ProteNova, Kagawa, Japan) with 4 μg of anti-His antibody. Half of the beads were used for western blotting. The RNAs co-precipitated with the beads were extracted from the remainder of the beads using ISOSPIN Cell&Tissue RNA. Following the reverse transcription reaction with random primers, qPCR was performed. The experiments were repeated three times.

2.10 Statistical analysis

Data are expressed as the mean ± standard deviation (SD). Following the F-test to analyze variances, the unpaired two-sided Student's *t*-test was used to determine the statistical significance of the mean values of the luminescent intensity between the two conditions (Figs. 1C, S1, S6B, and C). Dunnett's multiple comparison tests were performed for the multiple

comparisons against the control condition after one-way analysis of variance tests (ANOVA) (Figs.2A, B, C, 3B, and S6A). Following ANOVA, the Tukey−Kramer test was used for multiple comparisons of statistical significance (Figs. 2D, 5B, S2A, B, and S6D). Statistical analyses were performed with GraphPad Prism: *: $p \leq 0.05$, **: $p \leq 0.01$, ***: $p \leq 0.001$, and ****: $p < 0.0001$.

3. Results

3.1 Establishment of the minigenome of orthonairoviruses.

Our orthonairovirus minigenome consists of three components: a reporter RNA encoding secNluc and two plasmids expressing viral L or N (Fig. 1A). We employed the *in vitro*-transcribed RNA for the reporter to avoid non-specific transcription/translation of positive-strand RNA from the plasmid. The reporter RNA was designed with NCS of the CCHFV Hoti strain L segment (Duh et al., 2008) or the HAZV JC280 strain S segment (Begum et al., 1970) because of the high reporter activities in previous reports (Bergeron et al., 2010; Matsumoto et al., 2019). After the transfection of the reporter RNA to cells infected with a helper virus, a marked increase in the luciferase signal was observed (Fig. S1), indicating that reporter RNAs were functionally sufficient. Next, we confirmed the protein expression from the constructed plasmids, and the tagged proteins were expressed in the expected size (Fig. 1B). Transfection of the reporter RNAs induced a significant increase in luciferase activity in cells transfected with the expression plasmids (Fig. 1C). These results showed that our minigenome worked well.

3.2 Analysis of the requirements of minigenome replication.

We analyzed the requirements for viral replication using the established minigenome. HEK293T cells with both L and N plasmids showed the highest luciferase activity in both CCHFV and

194 HAZV minigenome, whereas transfection with only L plasmid slightly increased luciferase
195 activity (Fig. 2A). The abundance of positive strands of the reporter RNA significantly increased
196 in cells with both L and N (Fig. 2B), consistent with the results of the luciferase activity. These
197 results indicated that both L and N were required for the efficient transcription of orthonairovirus
198 reporter RNAs.
199
200 Next, we analyzed minigenome replication in heterogeneous combinations of L, N, and the
201 reporter RNA between CCHFV and HAZV. The cells with the homogenous pair of L and N
202 proteins showed significantly higher luciferase activity than the negative control cells, while cells
203 with heterogeneous pairs did not (Fig. 2C). In contrast, the reporter RNAs did not require a protein
204 pair that was homogenous with the RNA (Figs. 2C and S2A). A reporter RNA with taxonomically
205 distant virus sequences did not show the sign of replication by the CCHFV L and N proteins (Fig.
206 S2B), suggesting a conserved motif in the non-coding sequences for the orthonairovirus
207 replication.
208
209 To further analyze the requirement for viral replication, we attempted to mutate a protein motif.
210 The active site of RdRp in L was structurally predicted and analyzed using transcriptionally
211 competent virus-like particles (Devignot et al., 2015; Mirza et al., 2019). The RdRp mutation
212 significantly decreased luciferase activity (Figs. 2D and S3). As expected, our minigenome
213 system was capable of analyzing the requirements for viral replication by mutagenesis.
214
215 *3.3 FDA-approved drug screening by CCHFV minigenome system.*
216 To explore the inhibitors of CCHFV replication, a library of 630 FDA-approved compounds were
217 screened. We employed BHK-21 cells for this screening because of the ease of handling. As

shown in Fig. 3A, the cells with the CCHFV minigenome were cultured in the presence of 20 μg/ml compounds or ribavirin as a positive control. The Z-factors of the three independent experiments were 0.79, 0.64, and 0.85, which were reliable levels, and the data were correlated and distributed similarly (Fig. S4). We set the cut-off values to $p < 0.05$ in comparison to DMSO-treated cells for luciferase activity and Log_{10} 8.1 for cell viability, approximately 40% cell viability of the DMSO-treated cells. Fourteen compounds (Table 1) significantly decreased the luciferase activity among the tested compounds and had little influence on cell viability (Fig. 3B and Supplemental data).

3.4 Validation of the inhibitor candidates and their derivatives.

Considering the adverse effects and ease of availability, we selected six compounds and tested their dose-response and cytotoxicity (Figs. 4A and S5). We also analyzed the derivatives of some compounds: minocycline hydrochloride, tigecycline (tetracycline antibiotics), and ergotamine tartrate (ergot alkaloid). Alfacalcidol and ergotamine tartrate showed strong cytopathic effect at 50 μM (Fig. S5) and were excluded from the analysis. Tetracycline, doxycycline hyclate, minocycline hydrochloride, and promethazine hydrochloride showed activity equivalent to that of ribavirin (Fig. 4A). Dihydroergotamine mesylate and nisoldipine showed differences in the activity between CCHFV and HAZV: 50% inhibition at 8.58 μM v.s. 23.8 μM and 12.7μM v.s. > 50μM, respectively. Tigecycline worked on both minigenome and showed 50% inhibition at a concentration lower than 10 μM (Fig. 4A).

We validated the effect of these compounds on the replication of the infectious virus by using HAZV. Tigecycline showed 50% inhibition at 6.40 μM, which reflected the results of the minigenome (Fig. 4B). Dihydroergotamine mesylate showed 50% inhibition at 18.6 μM, which

was similar to the result of the minigenome (Fig. 4B).

3.5 Effect of tigecycline on the interaction between N and viral RNA.

We attempted to analyze the mechanism of inhibition by tigecycline. A reporter assay showed a limited effect of tigecycline on a protein expression from the transfected plasmid (Fig. S6A). In cells transfected with minigenome or infected with HAZV, RT-qPCR showed decreased RNA abundance in the presence of tigecycline (Fig. S6B and C). These results indicated an influence on the transcription of the viral genome. The combination treatment of tigecycline and ribavirin did not compete with each other, which suggested independent targets of inhibition between them (Fig. S6D). Previously, Sharifi *et al* virtually screened compounds binding to pockets of CCHFV N (Sharifi et al., 2017), which were predicted to bind viral RNA (Jeeva et al., 2017b; Wang et al., 2016). Intriguingly, several compounds, including doxycycline and minocycline, overlapped with our candidates. Therefore, we analyzed the influence of tigecycline on the interaction between N and viral RNA. We mixed the cell lysates expressing viral proteins with an equivalent amount of the reporter RNA in the presence or absence of tigecycline and precipitated N protein. Equivalent amounts of N and L precipitated in the presence of the compounds, suggesting a limited influence on the protein-protein interactions (Fig. 5A). In contrast, treatment with tigecycline significantly decreased the RNA abundance of the reporter RNA that was co-precipitated (Fig. 5B). These results showed the inhibition of the interaction between N and RNA by tigecycline.

4. Discussion

Our reporter RNA with the CCHFV NCS was replicated under heterogeneous HAZV infection as a helper virus (Fig. S1). Replication of reporter RNAs did not require the expression of

homogenous viral proteins (Figs. 2C and S2A). A previous study showed the importance of conserved promoter elements, which were conserved in our reporter RNAs (Fig. S7), for the replication of the HAZV minigenome (Matsumoto et al., 2019). The requirement of NCSs may be flexible except for conserved terminal sequences. In contrast, the reporter RNA did not replicate in the heterogeneous protein pairs (Fig. 2C), indicating that the homogenous interaction between L and N is essential for the formation of a functional complex for genome replication.

Our screening identified 14 compounds as CCHFV inhibitor candidates (Fig. 3B and Table 1), some of which overlapped with screenings against other viruses in *Bunyavirales* (Benedict et al., 2015; Li et al., 2019). Alfacalcidol, an analog of vitamin D, influences cellular calcium homeostasis. Calcium metabolism participates in the regulation of endoplasmic reticulum stress response and apoptotic signaling (Zhou et al., 2009) and its disturbance could result in the inhibition of CCHFV replication. Nisoldipine, a calcium channel blocker, was shown to inhibit multiple steps of Dabie bandavirus, or SFTSV, replication (Li et al., 2019; Urata et al., 2021) and our data suggested a similar effect on CCHFV replication. A study with the influenza A virus showed that itraconazole, an azole antifungal, induced endolysosomal cholesterol storage, resulting in decreased viral replication (Schloer et al., 2019). CCHFV also required cholesterol for its replication (Simon et al., 2009), and ketoconazole might similarly inhibit CCHFV replication.

Our results identified tetracyclines, especially tigecycline, as potent inhibitors of orthonairoviruses *in vitro* (Fig. 4). Tigecycline dissociated N and viral RNA (Fig. 5). Wang *et al* proposed a model of RNA binding of N protein via positively charged patches and a groove between these patches (Wang et al., 2016). The occupation of this groove, which is predicted as a

290 binding target of tetracyclines (Sharifi et al., 2017), may result in the inhibition of the interaction
291 and viral replication (Fig. 5). The interaction between N and RNA participates in multiple steps
292 of the viral life cycle. It was suggested that N is involved in 5' Cap-snatching via the interaction
293 with 5' Cap and the 5' sequences of the cellular mRNA (Knipe and Howley, 2013; Mir et al.,
294 2008). However, the RNA used in our RNA-immune precipitation was synthesized without 5'
295 Cap. The 5' Cap-binding activity was not necessary to be affected by tigecycline. A previous study
296 showed that N facilitated the dissociation of the RNA panhandle, which supports viral RNA
297 transcription (Mir and Panganiban, 2006). In addition, N promoted viral protein translation by
298 recruiting the eukaryotic initiation factor (Jeeva et al., 2017a). Tigecycline may disturb these steps
299 of viral transcription and translation. Tetracyclines are antibiotics and inhibitors of the 30S subunit
300 of bacterial ribosomes (Brodersen et al., 2000), although recent studies have reported the effects
301 on mammalian and mitochondrial ribosomes (Chatzispyrou et al., 2015; Mortison et al., 2018).
302 CCHFV mRNAs might be more sensitive to translation distraction than cellular mRNAs. These
303 results showed that the interaction between N and viral RNA could be a target of antiviral agents,
304 such that the design of derivatives with a stronger binding affinity will contribute to the
305 development of CCHFV antiviral in future studies.
306
307 We showed the concentration of 50% inhibition of tigecycline was lower than 10 μM, which was
308 somehow competitive with that of favipiravir (T705), 7.0 μM (Oestereich et al., 2014). However,
309 a previous study showed the *in vivo* concentration of tigecycline in serum was ranged from 1.32
310 mg/L (2.25 μM) to 0.22 mg/L (0.37 μM) after single 100 mg administration (Rodvold et al., 2006),
311 which did not meet the level of 50% inhibition. It may be acceptable to increase the administration
312 dose in this case of lethal pathogen infection, but, careful validation of the side effect would be
313 required. A combinational treatment of tigecycline and nucleotide analogs might be beneficial, as

our data suggested they have independent targets (Fig. S6D).

In this study, we developed the minigenome of orthonairoviruses and demonstrated its validity in antiviral screening. We identified tigecycline as a potent antiviral against CCHFV via the dissociation of N and viral RNA. Future validation with *in vivo* and the design of the chemical derivatives with stronger levels of activity will facilitate the development of the specific antiviral against CCHFV and its clinical applications in patients.

5. Acknowledgments

We would like to thank Prof. Hewson (Public Health England's Porton Down Institute, England) for providing us HAZV JC280 strain kindly. We greatly applicate Ms. Chloe Nagasawa (University of Texas Medical Branch at Galveston) reviewing the manuscript. We would like to thank Editage (www.editage.com) for English language editing.

This work is supported by Grants-in-Aid for Scientific Research (19K22353, 20H03136, 21K19191, 21K20761, 19K21260, and 20K07516) from the Ministry of Education, Culture, Sports, Sciences and Technology of Japan, and a grant for research on Japan Program for Infectious Diseases Research and Infrastructure from AMED (21fm0208101j0005, 21jm0210072h0003 and 21fk0108614h0301).

Figure legends

Figure 1. Establishment of the minigenome system of orthonairoviruses.

A: Schematic diagram of the minigenome system. The reporter RNA consists of a reverse complement sequence of secNluc CDS with 5' and 3' NCSs of CCHFV or HAZV genomic RNA. For the expression of viral L and N, the plasmids with pCAG-Hyg backbone were constructed. **B:** Western-blotting images of the HEK293T cells co-transfected with/without the L and N expression plasmids. Left panels: CCHFV plasmids, Right panels: HAZV plasmids. **C:** Positive strand synthesis and translation of the orthonairovirus minigenome. HEK293T cells co-transfected with (black) or without (white) the viral protein expression plasmids were transfected with the reporter RNA. The luciferase activity was measured at 24 and 48 h.p.t. Left: CCHFV minigenome, Right: HAZV minigenome.

Figure 2. Analysis of the requirements of the minigenome replication.

A-B: Protein requirements of minigenome replication. HEK293T cells were mock-transfected (white bars) or transfected with L (gray) or N (gray-striped), or co-transfected with both of them (black). After the reporter RNA transfection, the luciferase activity of the supernatants (**A**) and the relative RNA abundance of the luciferase gene against GAPDH (**B**) were measured. **C:** Heterogeneous combinations of proteins and RNA in the minigenome. The HEK293T cells co-transfected with the L and N expression plasmids of CCHFV (C) or HAZV (H) were transfected with the reporter RNAs of the CCHFV L segment (left) or HAZV S segment (right). Minigenome replication was evaluated via the luciferase assay. **D:** Mutagenesis of the RdRp motif of HAZV L. The HEK293T cells were transfected with the plasmids expressing N and L wild type (WT, black) or L RdRp mutant (⊿RdRp, gray). The minigenome replication was evaluated via the luciferase assay after the reporter RNA transfection.

Figure 3. FDA-approved drug screening with CCHFV minigenome.

A: Time course of the experiment. BHK-21 cells were transfected with the CCHFV minigenome on 96 well plates, and then the compound library was added at the final concentration of 20 μg/ml. Following incubation for 48 h, the minigenome replication or cell viability was evaluated via the luciferase assay or the resazurin assay, respectively. **B:** Results of drug screening plotted as dot plots. The top graph shows a plot of Log_{10} (Cell viability) in the x-axis and Log_{10} (Luciferase activity) in the y-axis. The bottom graph shows a plot of compound ID in the x-axis and $-log_{10}$ (p-value) in the y-axis. DMSO- and ribavirin-treated wells were used as negative control (green) and positive control (orange), respectively. The compounds that passed the cut-off values (magenta) are shown as the inhibitor candidates.

Figure 4. Validation of the inhibitor candidates and their derivatives.

A: Dose-response of inhibitor candidates and their derivatives. BHK-21 cells were transfected with the CCHFV (black) or HAZV (white) minigenome, followed by the addition of the inhibitor candidates at a final concentration from 10-50 μM. Minigenome replication was evaluated via the luciferase assay and is shown as relative luciferase against DMSO-treated wells. The black and dotted lines indicate the non-linear regression of the dose-response. CCHFV50 or HAZV50 indicates concentration of 50% inhibition of each minigenome, respectively. **B:** Evaluation of the efficacy of the compounds against infectious HAZV replication. SW-13 cells were infected with HAZV at an MOI of 0.005, and viral replication under the compounds was evaluated by plaque assay and was shown as a relative virus titer against DMSO-treated wells. Gray lines indicate the concentration of the 50% inhibition of HAZV infection.

Figure 5. Analysis of the inhibitory mechanism of tigecycline

A-B: RNA immunoprecipitation of N protein under tigecycline. The cell lysates of HEK293T cells expressing CCHFV L and N were incubated with the reporter RNA under the presence or absence of ribavirin or tigecycline. After the immunoprecipitation of N, the L and N (**A**) and reporter RNA (**B**) were detected by western blotting or RT-qPCR against the luciferase gene, respectively. The representing image of the western-blotting is shown.

Figure S1. Reporter activity under the helper virus infection.

Replication of the reporter RNAs with a helper virus. BHK-21 cells were infected with HAZV at an MOI of 0.005 (black) or mock-infected (white). At 48 hours post-infection (h.p.i.), the cells were transfected with the reporter RNA and were cultured for 24 h. The expression of the luciferase protein was evaluated by the luciferase assay.

Figure S2. Reporter activity of the minigenome with variations.

A: The BHK-21 cells co-transfected with the L and N expression plasmids of CCHFV (C, Black bar) or HAZV (H, Gray bar) were further transfected with the mCherry-expressing reporter RNAs of the CCHFV L segment. Images of the control cells or cells showing mCherry signal were taken with ZOE fluorescent imager (Bio-rad). The fluorescent intensity of five independent images was measured with Image J (Schneider et al., 2012). **B:** Minigenome assay of lymphocytic choriomeningitis virus (LCMV) backbone (Urata et al., 2016). The BHK-21 cells were co-transfected with a plasmid encoding GFP-expressing reporter RNA of LCMV and the L and N expression plasmids of LCMV (LC, Black) or CCHFV (C, Gray). The fluorescent intensities were measured as described above.

Figure S3. Expression of CCHFV L and N with mutations.

Western blotting images of HEK293T cells co-transfected with L and N expression plasmids with or without ⊿RdRp mutation.

Figure S4. Data distributions of the FDA-approved drug library screening.

A: Data correlation between the experiments. The Log_{10} (Luciferase activity) was normalized as robust z-scores and plotted as dot plots. DMSO- or ribavirin-treated wells were used as a

negative control (green) and positive control (orange), respectively. The compounds that passed the cut-off points (magenta) are shown as inhibitor candidates. **B:** Histogram representing the distribution of reporter activity or cell viability of the drug screening. The robust z-scores were used to bin the range of values (x-axis, bin center). The counts of the compounds falling into each interval were shown (y-axis, number). blue: Experiment 1, green: Experiment 2, orange: Experiment 3.

Figure S5. Cell viability under the presence of the inhibitor candidates.

The compounds were added to the culture medium of BHK-21 cells with 1% (v/v) DMSO at a final concentration from 0 to 200 μM. Resazurin assay was conducted at 48 h.p.t., and the relative cell viability (%) against the signal of the control wells was calculated. A fitting curve with non-linear regression was conducted based on triplicate results, and the 50% cytotoxic concentration (CC50) was measured using GraphPad Prism. Selectivity indexes (SI) were calculated from the CC50 divided by the concentration of 50% inhibition of CCHFV minigenome.

Figure S6. Effect of tigecycline on the CCHFV minigenome system.

A: Effect of tigecycline on the expression of the plasmid-derived protein. BHK-21 cells were transfected with pCAG-Hyg-GFP-T2A-CCHFV N. After 6h of incubation, the culture medium was replaced with that contains ribavirin or tigecycline. After 48 h of culture, fluorescent intensities of the expressed GFP were measured with SpectraMax iD5. **B:** Effect on minigenome replication. HEK293T cells with the CCHFV minigenome were cultured with or without the 25 μM tigecycline for 48 h. Total RNA was extracted with ISOGEN II (Nippon Gene). RNA abundance was measured using strand-specific RT-qPCR. **C:** Effect on infectious

virus replication. SW-13 cells infected with HAZV at an MOI of 0.5 were cultured with or without 25 μM tigecycline for 24 h. Total RNA was extracted from the cells with ISOSPIN Cell&Tissue RNA. Following the reverse transcription reaction with random primers, qPCR was conducted with primers targeting HAZV S segment (Fw: 5'cgcctgctgaggcattact3', Rv: 5'ctggtgtactccccaatgga3'), M seg (Fw: 5'aatctgaaggaccggttgtg3', Rv: 5'tttgtcaacctcaacggtca3'), L segment (Fw: 5'atcagcgacttctttaggcg3', Rv: 5'attgcctaggcttccagcac3') and GAPDH. The RNA abundance of each segment against GAPDH is shown. **D:** Combination treatment of tigecycline and ribavirin. BHK-21 cells with CCHFV minigenome were treated with 4 μM tigecycline and/or 32 μM ribavirin. Luciferase activity was measured at 48 h.p.t., and relative luciferase signal against DMSO treated sample was calculated.

Figure S7. Comparison of NCS between reporter RNAs.

Schematic diagram of the conserved terminal sequence of the reporter RNAs of CCHFV Hoti L segment, HAZV JC280 S segment, and LCMV Armstrong S segment (Outgroup). Magenta: conserved nucleotide sequences.

References

Akıncı, E., Bodur, H., Leblebicioglu, H., 2013. Pathogenesis of Crimean-Congo Hemorrhagic Fever. Vector-Borne Zoonotic Dis. 13, 429–437. https://doi.org/10.1089/VBZ.2012.1061

Altaf, A., Luby, S., Jamil, A., Najam, A., Aamir, Z., Khan, J., Mirza, S., McCormick, J., Fisher-Hoch, S., 1998. Outbreak of Crimean-Congo haemorrhagic fever in Quetta, Pakistan: contact tracing and risk assessment. Trop. Med. Int. Heal. 3, 878–882. https://doi.org/10.1046/J.1365-3156.1998.00318.X

Begum, F., Wisseman, C.L., Casals, J., 1970. TICK-BORNE VIRUSES OF WEST PAKISTAN: II. HAZARA VIRUS, A NEW AGENT ISOLATED FROM IXODES REDIKORZEVITICKS FROM THE KAGHAN VALLEY, W. PAKISTAN. Am. J. Epidemiol. 92, 192–194. https://doi.org/10.1093/OXFORDJOURNALS.AJE.A121197

Benedict, A., Bansal, N., Senina, S., Hooper, I., Lundberg, L., de la Fuente, C., Narayanan, A., Gutting, B., Kehn-Hall, K., 2015. Repurposing FDA-approved drugs as therapeutics to treat Rift Valley fever virus infection. Front. Microbiol. 0, 676. https://doi.org/10.3389/FMICB.2015.00676

Bente, D.A., Forrester, N.L., Watts, D.M., McAuley, A.J., Whitehouse, C.A., Bray, M., 2013. Crimean-Congo hemorrhagic fever: History, epidemiology, pathogenesis, clinical syndrome and genetic diversity. Antiviral Res. 100, 159–189. https://doi.org/10.1016/J.ANTIVIRAL.2013.07.006

Bergeron, É., Albariño, C.G., Khristova, M.L., Nichol, S.T., 2010. Crimean-Congo Hemorrhagic Fever Virus-Encoded Ovarian Tumor Protease Activity Is Dispensable for Virus RNA Polymerase Function. J. Virol. 84, 216–226. https://doi.org/10.1128/JVI.01859-09

Brodersen, D.E., Clemons, W.M., Carter, A.P., Morgan-Warren, R.J., Wimberly, B.T.,

Ramakrishnan, V., 2000. The Structural Basis for the Action of the Antibiotics Tetracycline, Pactamycin, and Hygromycin B on the 30S Ribosomal Subunit. Cell 103, 1143–1154. https://doi.org/10.1016/S0092-8674(00)00216-6

Chatzispyrou, I.A., Held, N.M., Mouchiroud, L., Auwerx, J., Houtkooper, R.H., 2015. Tetracycline Antibiotics Impair Mitochondrial Function and Its Experimental Use Confounds Research. Cancer Res. 75, 4446–4449. https://doi.org/10.1158/0008-5472.CAN-15-1626

Chung, N., Zhang, X.D., Kreamer, A., Locco, L., Kuan, P.-F., Bartz, S., Linsley, P.S., Ferrer, M., Strulovici, B., 2008. Median Absolute Deviation to Improve Hit Selection for Genome-Scale RNAi Screens: J. Biomol. Screen. 13, 149–158. https://doi.org/10.1177/1087057107312035

Dai, S., Deng, F., Wang, H., Ning, Y., 2021. Crimean-Congo Hemorrhagic Fever Virus: Current Advances and Future Prospects of Antiviral Strategies. Viruses 13, 1195. https://doi.org/10.3390/V13071195

Devignot, S., Bergeron, E., Nichol, S., Mirazimi, A., Weber, F., 2015. A Virus-Like Particle System Identifies the Endonuclease Domain of Crimean-Congo Hemorrhagic Fever Virus. J. Virol. 89, 5957–5967. https://doi.org/10.1128/JVI.03691-14

Dowall, S.D., Findlay-Wilson, S., Rayner, E., Pearson, G., Pickersgill, J., Rule, A., Merredew, N., Smith, H., Chamberlain, J., Hewson, R., 2012. Hazara virus infection is lethal for adult type I interferon receptor-knockout mice and may act as a surrogate for infection with the human-pathogenic Crimean–Congo hemorrhagic fever virus. J. Gen. Virol. 93, 560–564. https://doi.org/10.1099/VIR.0.038455-0

Duh, D., Nichol, S.T., Khristova, M.L., Saksida, A., Hafner-Bratkovič, I., Petrovec, M., Dedushaj, I., Ahmeti, S., Avšič-Županc, T., 2008. The complete genome sequence of a

382 Crimean-Congo Hemorrhagic Fever virus isolated from an endemic region in Kosovo.
383 Virol. J. 2008 51 5, 1–6. https://doi.org/10.1186/1743-422X-5-7
384 Flick, R., Flick, K., Feldmann, H., Elgh, F., 2003. Reverse Genetics for Crimean-Congo
385 Hemorrhagic Fever Virus. J. Virol. 77, 5997–6006.
386 https://doi.org/10.1128/JVI.77.10.5997-6006.2003
387 Hawman, D.W., Haddock, E., Meade-White, K., Williamson, B., Hanley, P.W., Rosenke, K.,
388 Komeno, T., Furuta, Y., Gowen, B.B., Feldmann, H., 2018. Favipiravir (T-705) but not
389 ribavirin is effective against two distinct strains of Crimean-Congo hemorrhagic fever
390 virus in mice. Antiviral Res. 157, 18–26.
391 https://doi.org/10.1016/J.ANTIVIRAL.2018.06.013
392 Hoenen, T., Groseth, A., de Kok-Mercado, F., Kuhn, J.H., Wahl-Jensen, V., 2011.
393 Minigenomes, transcription and replication competent virus-like particles and beyond:
394 Reverse genetics systems for filoviruses and other negative stranded hemorrhagic fever
395 viruses. Antiviral Res. 91, 195–208. https://doi.org/10.1016/J.ANTIVIRAL.2011.06.003
396 Huber, P.J., Rochetti, E.M., 2009. Robust Statistics, 2nd ed. ed. Wiley.
397 Jasenosky, L.D., Neumann, G., Kawaoka, Y., 2010. Minigenome-based reporter system suitable
398 for high-throughput screening of compounds able to inhibit Ebolavirus replication and/or
399 transcription. Antimicrob. Agents Chemother. 54, 3007–3010.
400 https://doi.org/10.1128/AAC.00138-10
401 Jeeva, S., Cheng, E., Ganaie, S.S., Mir, M.A., 2017a. Crimean-Congo Hemorrhagic Fever Virus
402 Nucleocapsid Protein Augments mRNA Translation. J. Virol. 91.
403 https://doi.org/10.1128/JVI.00636-17
404 Jeeva, S., Pador, S., Voss, B., Ganaie, S.S., Mir, M.A., 2017b. Crimean-Congo hemorrhagic
405 fever virus nucleocapsid protein has dual RNA binding modes. PLoS One 12, e0184935.

https://doi.org/10.1371/JOURNAL.PONE.0184935

Johnson, S., Henschke, N., Maayan, N., Mills, I., Buckley, B.S., Kakourou, A., Marshall, R., 2018. Ribavirin for treating Crimean Congo haemorrhagic fever. Cochrane Database Syst. Rev. 2018. https://doi.org/10.1002/14651858.CD012713.PUB2

Knipe, D.M., Howley, P.M. (Eds.), 2013. Fields Virology, 6th Ed. ed. Lippincott Williams & Wilkins (LWW).

Li, H., Zhang, L.-K., Li, S.-F., Zhang, S.-F., Wan, W.-W., Zhang, Y.-L., Xin, Q.-L., Dai, K., Hu, Y.-Y., Wang, Z.-B., Zhu, X.-T., Fang, Y.-J., Cui, N., Zhang, P.-H., Yuan, C., Lu, Q.-B., Bai, J.-Y., Deng, F., Xiao, G.-F., Liu, W., Peng, K., 2019. Calcium channel blockers reduce severe fever with thrombocytopenia syndrome virus (SFTSV) related fatality. Cell Res. 2019 299 29, 739–753. https://doi.org/10.1038/s41422-019-0214-z

Macleod, J.M.L., Marmor, H., García-Sastre, A., Frias-Staheli, N., 2015. Mapping of the interaction domains of the Crimean–Congo hemorrhagic fever virus nucleocapsid protein. J. Gen. Virol. 96, 524–537. https://doi.org/10.1099/VIR.0.071332-0

Maltezou, H.C., Maltezos, E., Papa, A., 2009. Contact tracing and serosurvey among healthcare workers exposed to Crimean-Congo haemorrhagic fever in Greece. Scand. J. Infect. Dis. 41, 877–880. https://doi.org/10.3109/00365540903173619

Matsumoto, Y., Ohta, K., Kolakofsky, D., Nishio, M., 2019. A Minigenome Study of Hazara Nairovirus Genomic Promoters. J. Virol. 93. https://doi.org/10.1128/JVI.02118-18

Mir, M.A., Duran, W.A., Hjelle, B.L., Ye, C., Panganiban, A.T., 2008. Storage of cellular 5′ mRNA caps in P bodies for viral cap-snatching. Proc. Natl. Acad. Sci. 105, 19294–19299. https://doi.org/10.1073/PNAS.0807211105

Mir, M.A., Panganiban, A.T., 2006. The bunyavirus nucleocapsid protein is an RNA chaperone: Possible roles in viral RNA panhandle formation and genome replication. RNA 12, 272–

282. https://doi.org/10.1261/RNA.2101906

Mirza, M.U., Vanmeert, M., Froeyen, M., Ali, A., Rafique, S., Idrees, M., 2019. In silico structural elucidation of RNA-dependent RNA polymerase towards the identification of potential Crimean-Congo Hemorrhagic Fever Virus inhibitors. Sci. Reports 2019 91 9, 1–18. https://doi.org/10.1038/s41598-019-43129-2

Mortison, J.D., Schenone, M., Myers, J.A., Zhang, Z., Chen, L., Ciarlo, C., Comer, E., Natchiar, S.K., Carr, S.A., Klaholz, B.P., Myers, A.G., 2018. Tetracyclines Modify Translation by Targeting Key Human rRNA Substructures. Cell Chem. Biol. 25, 1506-1518.e13. https://doi.org/10.1016/J.CHEMBIOL.2018.09.010

Oestereich, L., Rieger, T., Neumann, M., Bernreuther, C., Lehmann, M., Krasemann, S., Wurr, S., Emmerich, P., de Lamballerie, X., Ölschläger, S., Günther, S., 2014. Evaluation of Antiviral Efficacy of Ribavirin, Arbidol, and T-705 (Favipiravir) in a Mouse Model for Crimean-Congo Hemorrhagic Fever. PLoS Negl. Trop. Dis. 8, e2804. https://doi.org/10.1371/JOURNAL.PNTD.0002804

Ozawa, M., Shimojima, M., Goto, H., Watanabe, S., Hatta, Y., Kiso, M., Furuta, Y., Horimoto, T., Peters, N.R., Hoffmann, F.M., Kawaoka, Y., 2013. A cell-based screening system for influenza A viral RNA transcription/replication inhibitors. Sci. Reports 2013 31 3, 1–7. https://doi.org/10.1038/srep01106

Paragas, J., Whitehouse, C.A., Endy, T.P., Bray, M., 2004. A simple assay for determining antiviral activity against Crimean-Congo hemorrhagic fever virus. Antiviral Res. 62, 21–25. https://doi.org/10.1016/J.ANTIVIRAL.2003.11.006

Rodvold, K.A., Gotfried, M.H., Cwik, M., Korth-Bradley, J.M., Dukart, G., Ellis-Grosse, E.J., 2006. Serum, tissue and body fluid concentrations of tigecycline after a single 100 mg dose. J. Antimicrob. Chemother. 58, 1221–1229. https://doi.org/10.1093/JAC/DKL403

454 Schloer, S., Goretzko, J., Kühnl, A., Brunotte, L., Ludwig, S., Rescher, U., 2019. The clinically
455 licensed antifungal drug itraconazole inhibits influenza virus in vitro and in vivo.
456 https://doi.org/10.1080/22221751.2018.1559709 8, 80–93.
457 https://doi.org/10.1080/22221751.2018.1559709
458 Schneider, C.A., Rasband, W.S., Eliceiri, K.W., 2012. NIH Image to ImageJ: 25 years of image
459 analysis. Nat. Methods. https://doi.org/10.1038/nmeth.2089
460 Scholte, F.E.M., Zivcec, M., Dzimianski, J. V., Deaton, M.K., Spengler, J.R., Welch, S.R.,
461 Nichol, S.T., Pegan, S.D., Spiropoulou, C.F., Bergeron, É., 2017. Crimean-Congo
462 Hemorrhagic Fever Virus Suppresses Innate Immune Responses via a Ubiquitin and
463 ISG15 Specific Protease. Cell Rep. 20, 2396–2407.
464 https://doi.org/10.1016/J.CELREP.2017.08.040
465 Sharifi, A., Amanlou, A., Moosavi-Movahedi, F., Golestanian, S., Amanlou, M., 2017.
466 Tetracyclines as a potential antiviral therapy against Crimean Congo hemorrhagic fever
467 virus: Docking and molecular dynamic studies. Comput. Biol. Chem. 70, 1–6.
468 https://doi.org/10.1016/J.COMPBIOLCHEM.2017.06.003
469 Simon, M., Johansson, C., Mirazimi, A., 2009. Crimean-Congo hemorrhagic fever virus entry
470 and replication is clathrin-, pH- and cholesterol-dependent. J. Gen. Virol. 90, 210–215.
471 https://doi.org/10.1099/VIR.0.006387-0
472 Spengler, J.R., Bergeron, É., Rollin, P.E., 2016. Seroepidemiological Studies of Crimean-Congo
473 Hemorrhagic Fever Virus in Domestic and Wild Animals. PLoS Negl. Trop. Dis. 10,
474 e0004210. https://doi.org/10.1371/JOURNAL.PNTD.0004210
475 Urata, S., Weyer, J., Storm, N., Miyazaki, Y., van Vuren, P.J., Paweska, J.T., Yasuda, J., 2016.
476 Analysis of Assembly and Budding of Lujo Virus. J. Virol. 90, 3257–3261.
477 https://doi.org/10.1128/JVI.03198-15/ASSET/7D289EAE-702F-471B-828B-

D568B6B65D33/ASSETS/GRAPHIC/ZJV9990914380003.JPEG

Urata, S., Yasuda, J., Iwasaki, M., 2021. Loperamide Inhibits Replication of Severe Fever with Thrombocytopenia Syndrome Virus. Viruses 2021, Vol. 13, Page 869 13, 869. https://doi.org/10.3390/V13050869

Wang, X., Li, B., Guo, Y., Shen, S., Zhao, L., Zhang, P., Sun, Y., Sui, S.F., Deng, F., Lou, Z., 2016. Molecular basis for the formation of ribonucleoprotein complex of Crimean-Congo hemorrhagic fever virus. J. Struct. Biol. 196, 455–465. https://doi.org/10.1016/J.JSB.2016.09.013

Watts, D.M., Ussery, M.A., Nash, D., Peters, C.J., 1989. Inhibition of Crimean-Congo Hemorrhagic Fever Viral Infectivity Yields in Vitro by Ribavirin. Am. J. Trop. Med. Hyg. 41, 581–585. https://doi.org/10.4269/AJTMH.1989.41.581

Welch, S.R., Scholte, F.E.M., Flint, M., Chatterjee, P., Nichol, S.T., Bergeron, É., Spiropoulou, C.F., 2017. Identification of 2′ -deoxy-2′ -fluorocytidine as a potent inhibitor of Crimean-Congo hemorrhagic fever virus replication using a recombinant fluorescent reporter virus. Antiviral Res. 147, 91–99. https://doi.org/10.1016/J.ANTIVIRAL.2017.10.008

Zhou, Y., Frey, T.K., Yang, J.J., 2009. Viral calciomics: Interplays between Ca2+ and virus. Cell Calcium 46, 1–17. https://doi.org/10.1016/J.CECA.2009.05.005

Hirano *et al*, Figure 1 (1.5 Column)

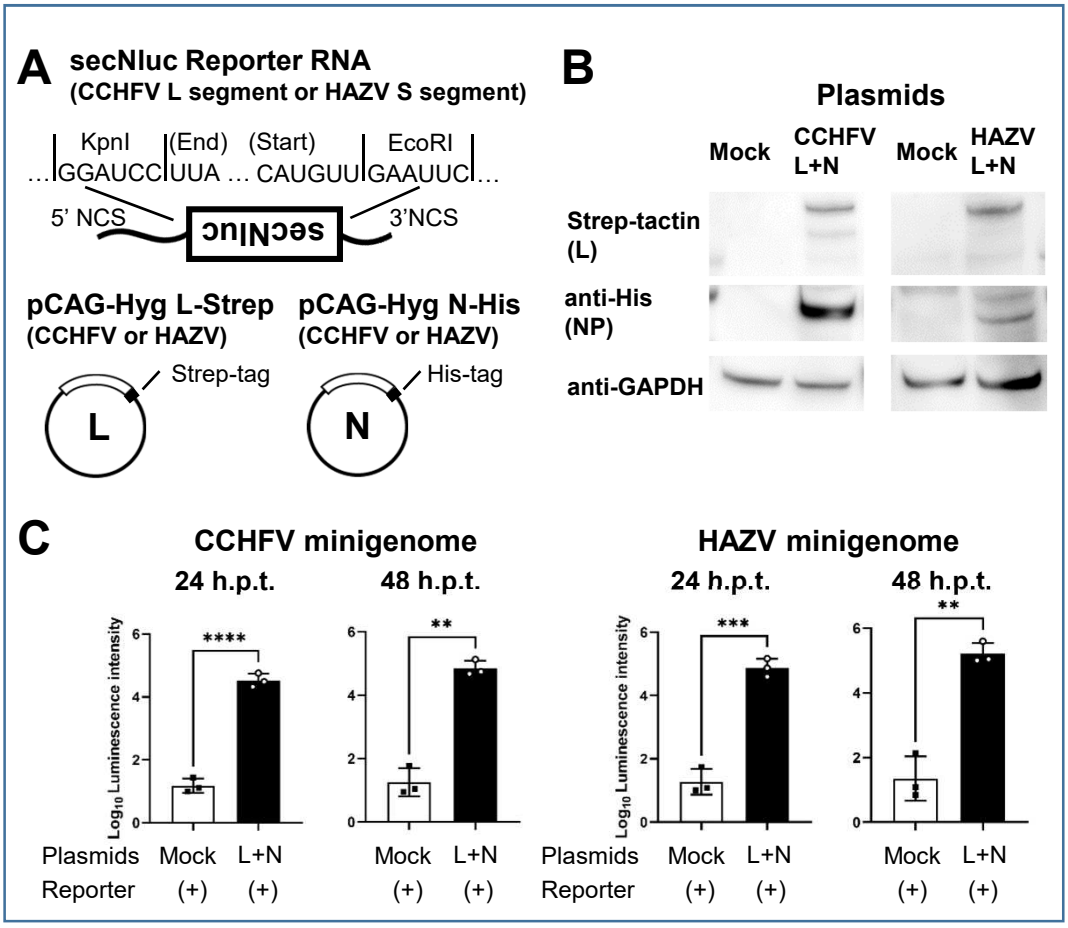

Hirano *et al*, Figure 2 (1.5 Column)

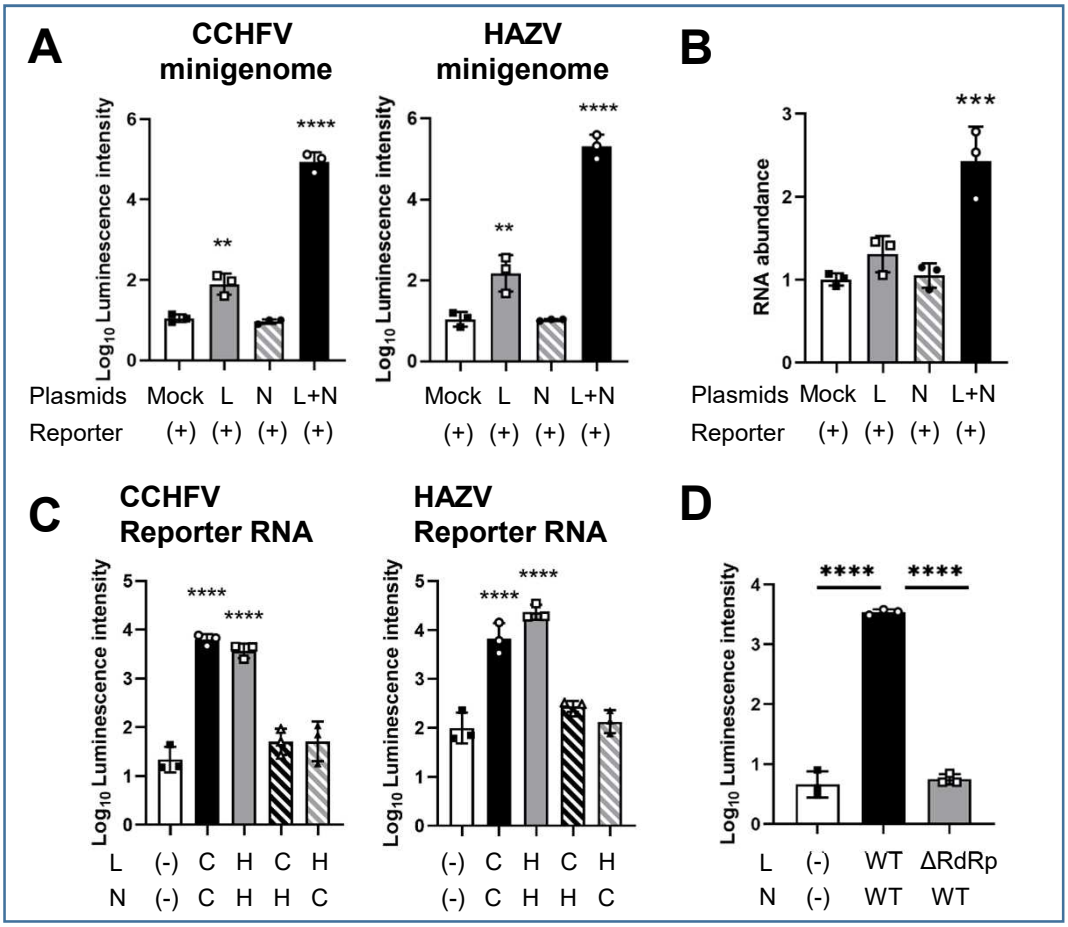

Hirano *et al*, Figure 3 (1.5 column, Color)

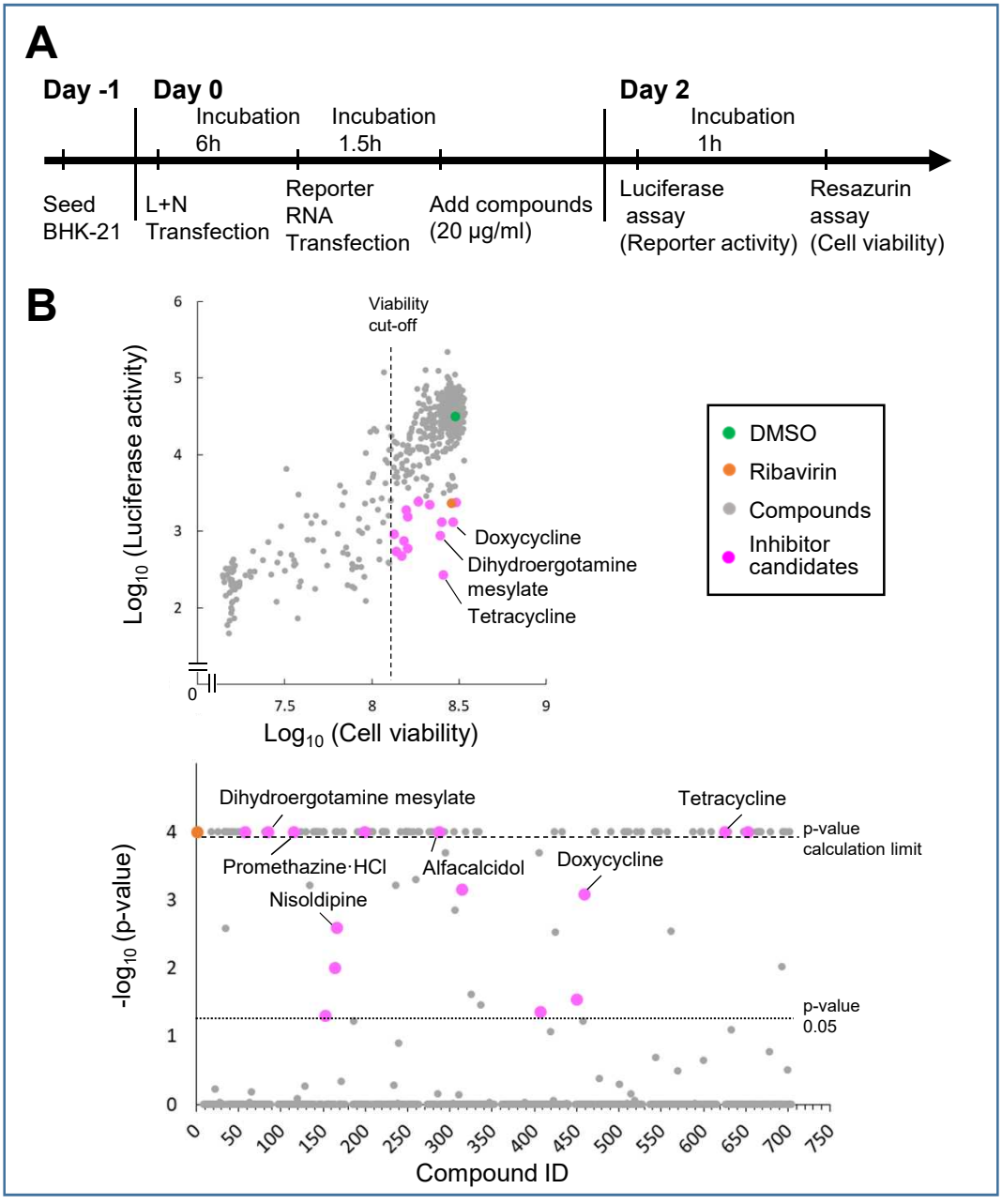

Hirano *et al*, Table 1

Table 1. List of the inhibitor candidates determined with the CCHFV minigenome.

Name	MW	CAS	Route	Medical use, Mechanism	Adverse effect, Toxicity
Tetracycline	444.4346	60-54-8	Oral, Parental, Topical	Antibiotics. Inhibitor of bacterial 30S ribosomal subunit.	Phototoxicity, stomach or bowel upsets
Lomofungin	314.2497	26786-84-5		Antifungal drug.	Not well characterized
Alfacalcidol	400.6371	41294-56-8	Oral	Analogue of vitamin D.	Hypocalcemia
Dihydroergocristine	611.7305	24730-10-7	Oral	Antihypertensive drug. Partial agonist activity on dopaminergic and alpha-adrenergic receptors.	Narrow therapeutic index
Ketoconazole	531.431	65277-42-1	(Oral), Topical	Antifungal drug. Inhibition of Ergosterol synthesis.	Hepatotoxicity, Cardiotoxicity in oral administration.
Dihydroergotamine mesylate	679.783	11032-41-0	Parental, Topical	Treatment of Migraine. Partial agonist activity on alpha-adrenergic receptors.	Dizziness, Narrow therapeutic index
Promethazine·HCl	320.88	58-33-3	Oral, Parental, Topical	Antihistamine medication. Control of parkisonism. Antagonist of Histamine H1 receptor.	Tardive dyskinesia, Drowsiness
Suramin	1291.232	129-46-4	Parental	Treatment of African trypanosomiasis.	Skin reaction, Nausea, Headache, Diarrhea
Doxycycline	444.4346	24390-14-5	Oral, Parental, Topical	Antibiotics. Inhibitor of bacterial 30S ribosomal subunit.	Phototoxicity, stomach or bowel upsets
Nisoldipine	388.4144	63675-72-9	Oral	Treatment of hypertension. Calcium channel inhibitor.	Ischemia, Myocardial infarction
Vitamin A acetate	328.4883	127-47-9	Oral	Vital roles in the retina formation and other epithelial differentiation. Formation of rhodopsin.	Headache, Rash
Dehydroepi androsterone	288.4244	53-43-0	Oral	Treatment of dyspareunia. C19 steroid and Precursor of steroid hormones (androstenedione and others).	Excessive testosterone
Ceftazidime	546.576	72558-82-8	Parental	Antibiotic for multi-drug resistant Gram-negative bacterial pathogens. Non-β-lactam β-lactamase inhibitor.	Abdominal cramps or tenderness, diarrhea
Entacapone	305.286	130929-57-6	Oral	Treatment of Parkinson's disease. Catechol-O-methyl transferase inhibitor.	Dizziness, nausea, diarrhea

Hirano *et al*, Figure 4 (1.5 column)

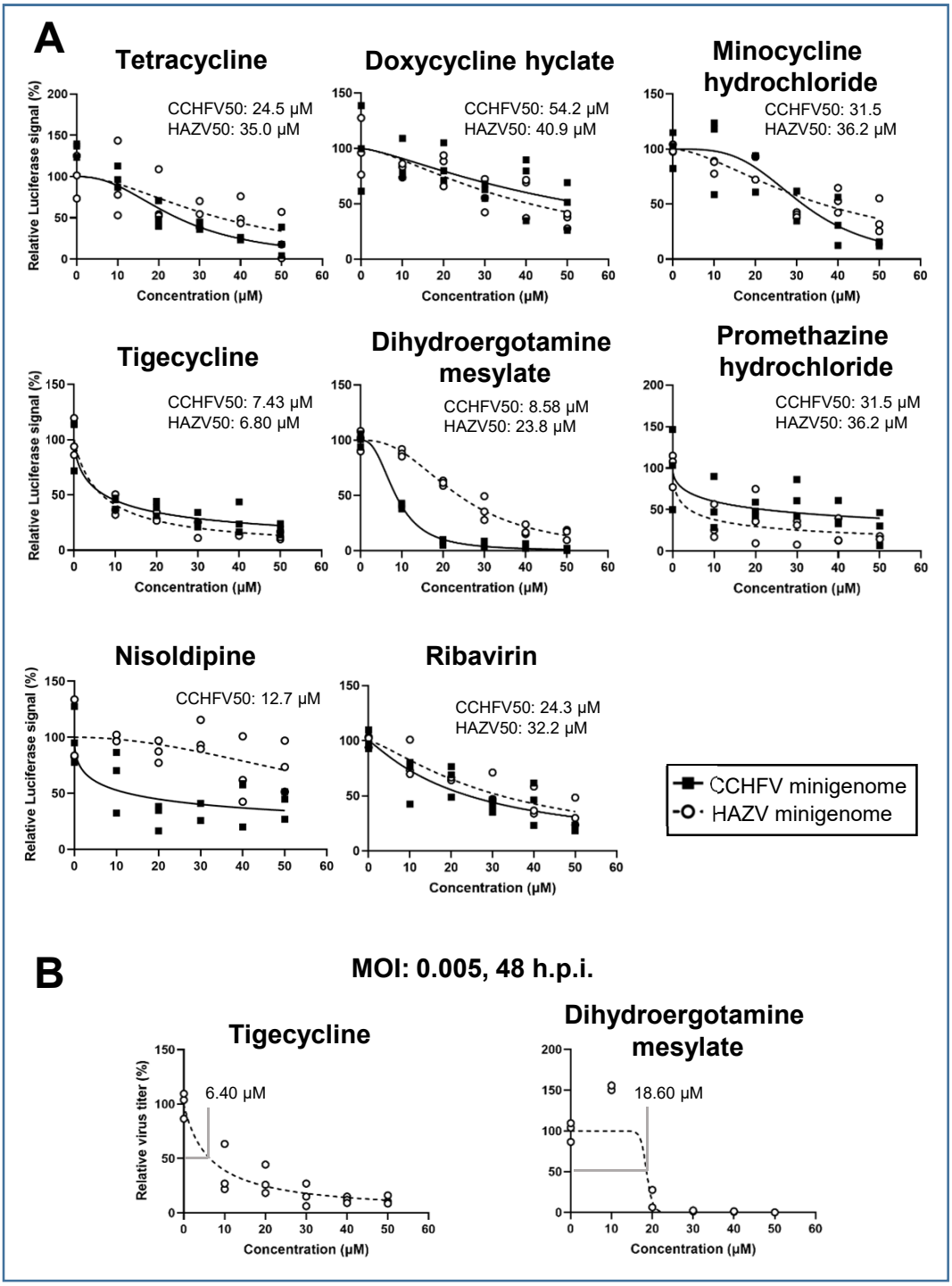

Hirano *et al*, Figure 5 (1.5 column)

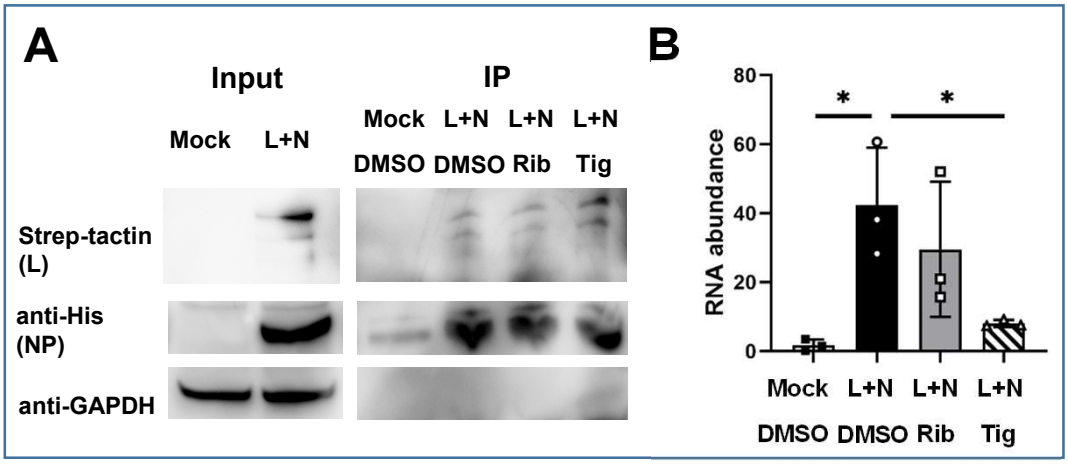

Hirano *et al*, Figure S1

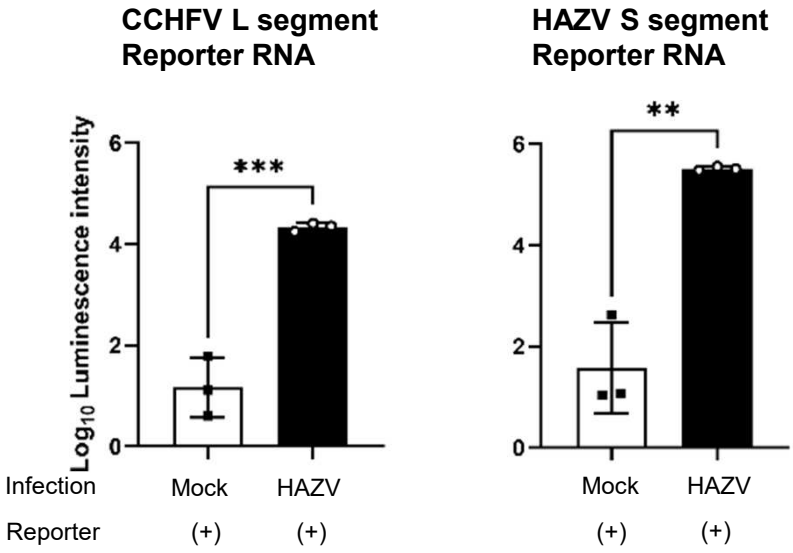

Hirano *et al*, Figure S2

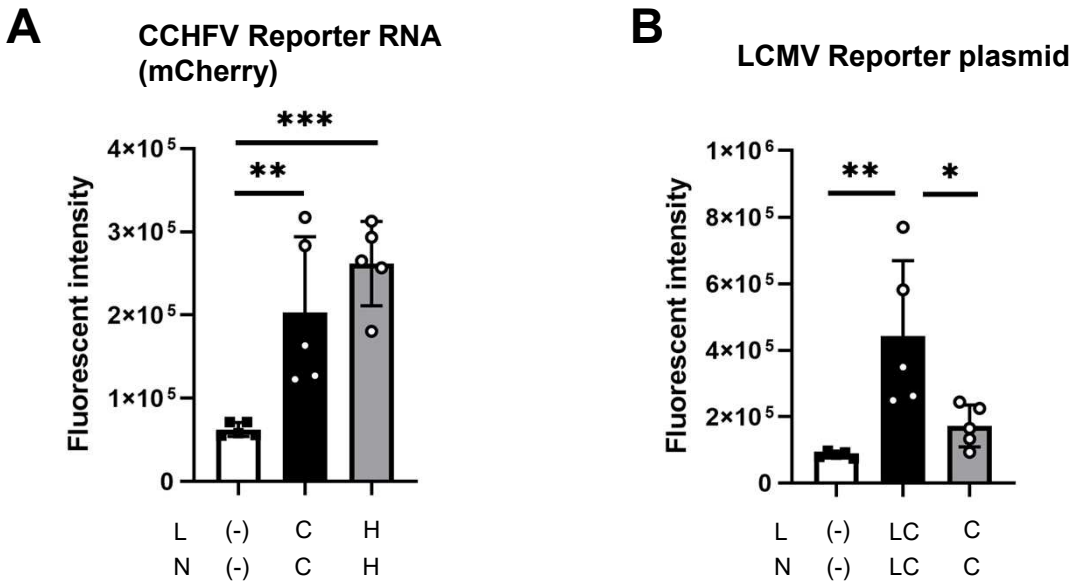

Hirano *et al*, Figure S3

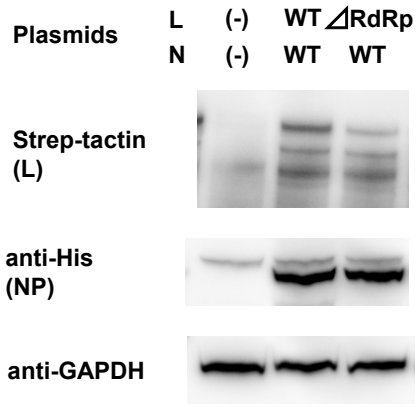

Hirano *et al*, Figure S4

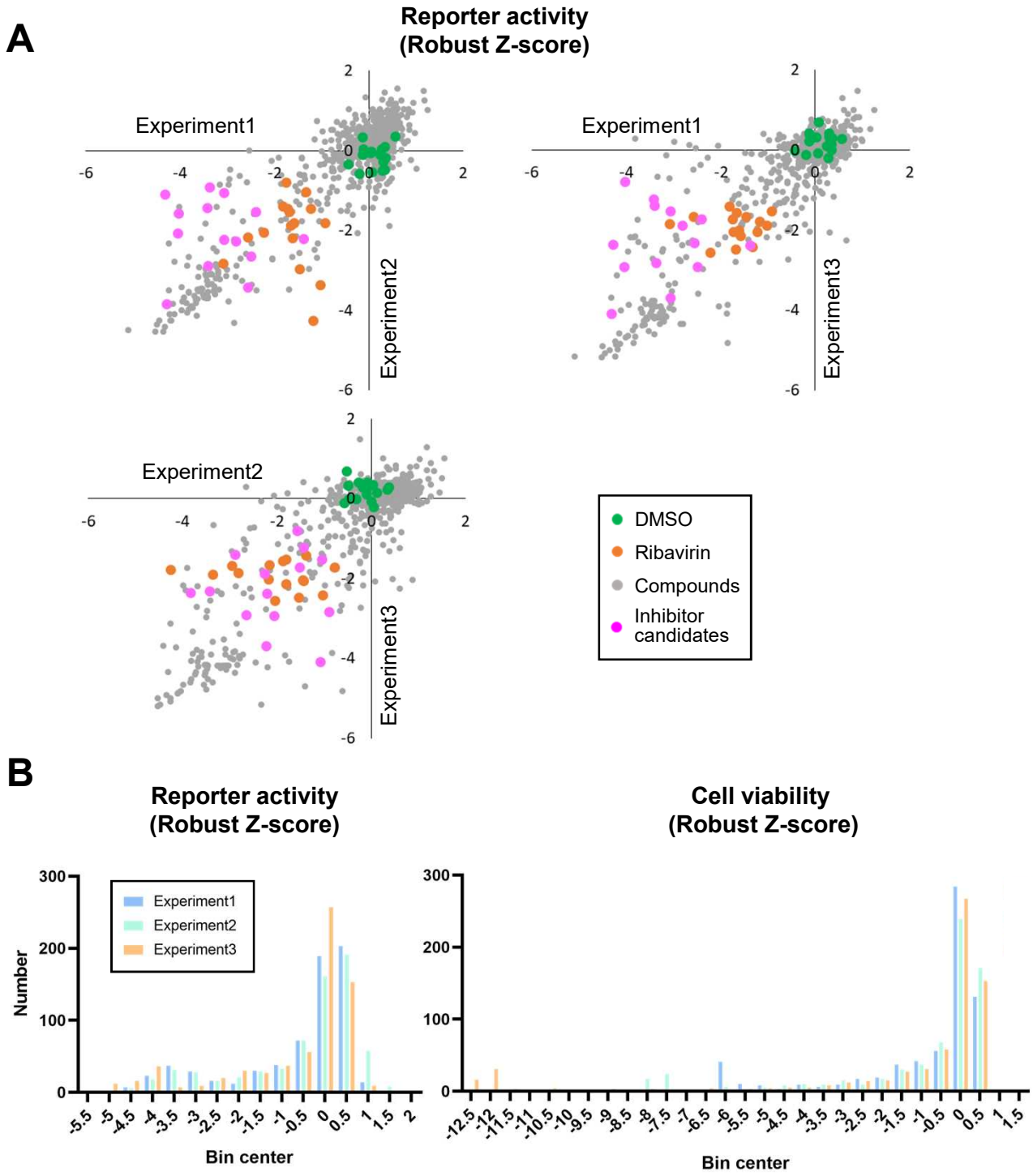

Hirano *et al*, Figure S5

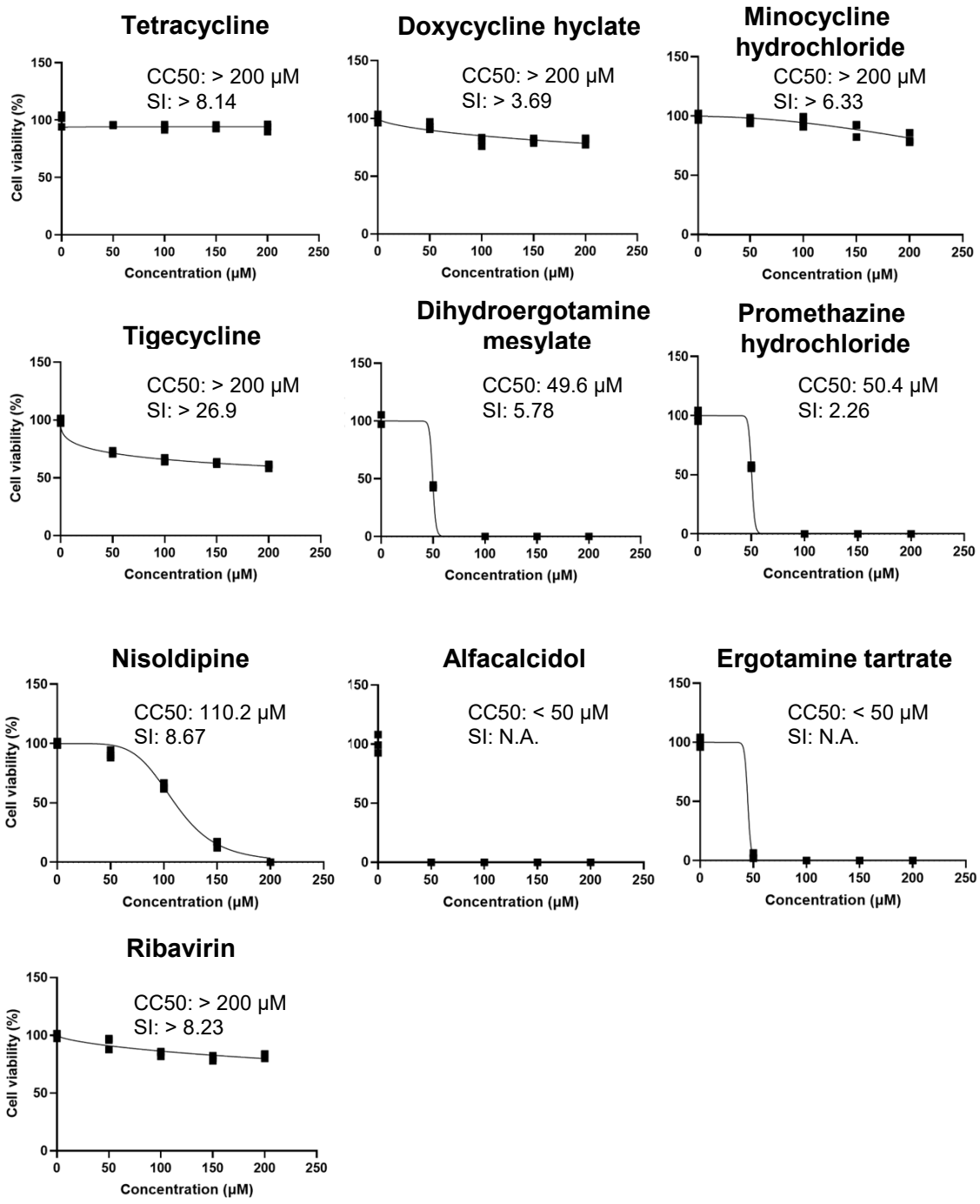

Hirano *et al*, Figure S6

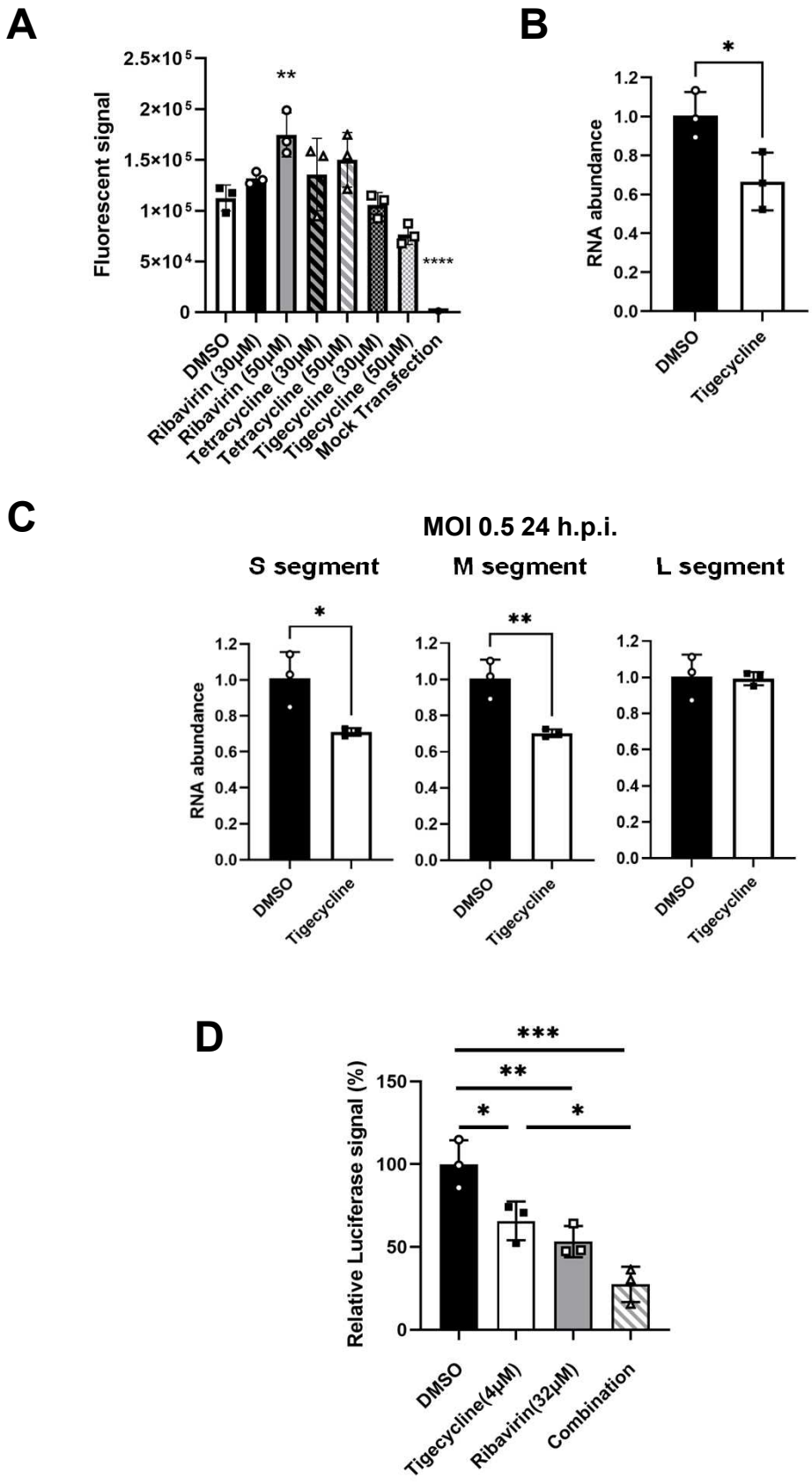

Hirano *et al*, Figure S7